

# Held-Suarez runs with CAM-SE: global axial angular momentum analysis using Eulerian & floating Lagrangian vertical coordinates



Peter Hjort Lauritzen<sup>1</sup> (pel@ucar.edu), J. Bacmeister<sup>1</sup>, M.A. Taylor<sup>2</sup>

<sup>1</sup> National Center for Atmospheric Research (NCAR), Boulder, Colorado, USA

<sup>2</sup> Sandia National Laboratories, Albuquerque, New Mexico, USA

## Introduction

The angular momentum of an atmosphere with respect to its rotation axis characterizes its rotary inertia and it is a fundamental physical quantity characterizing the general circulation of the atmosphere in question. When choosing the usual spherical coordinate system that rotates with the atmosphere and with coinciding rotation axes, the global axial angular momentum (AAM) can be separated into one part ( $M_r$ ) associated with the relative motion of the atmosphere with respect to the planets surface and another part ( $M_\Omega$ ) associated with the angular velocity  $\Omega$  ( $= 2\pi/d$ , where  $d$  is the length of the day) of the planet:

$$M = M_\Omega + M_r = \int_{\mathcal{D}} \Omega r^2 \cos^2 \theta dV + \int_{\mathcal{D}} u r \cos \theta dV. \quad (1)$$

where  $r$  is the radial distance from the center of the planet,  $u$  is the zonal velocity component,  $\theta$  the latitude,  $\lambda$  longitude,  $dV = r^2 \cos \theta d\lambda d\theta dr$  is an infinitesimal spherical volume, and  $\mathcal{D}$  is the global domain.

In the absence of any surface torque and zonal mechanical forcing, the hydrostatic primitive equations conserve the globally integrated AAM when assuming a constant pressure upper boundary [see, e.g., Staniforth and Wood, 2003]:

$$\frac{dM}{dt} = 0. \quad (2)$$

Typically numerical models are divided into a dynamical core ( $dyn$ ) that, roughly speaking, solves the equations of motion on resolved scales and physical parameterization that approximate sub-grid-scale processes ( $phys$ ). There can therefore be two sources/sinks of AAM:

$$\frac{dM}{dt} = \left(\frac{dM}{dt}\right)_{dyn} + \left(\frac{dM}{dt}\right)_{phys}. \quad (3)$$

In Held-Suarez setup ( $\left(\frac{dM}{dt}\right)_{phys}$  is simplified surface drag that acts on the velocity components only. Consequently it does not alter  $M_\Omega$  but only  $M_r$ . In Held-Suarez setup the sources/sinks of AAM in the dynamical core are due to numerical errors unless explicit or implicit diffusion is designed to mimic physical drag. In this study we assume that the dynamical core approximates the solution to the hydrostatic primitive equations and not any sub-grid-scale processes and should therefore, according to (2), not be a source/sink of global AAM.

In this study we are going to decompose  $\left(\frac{dM}{dt}\right)_{dyn}$  into two components

$$\left(\frac{dM}{dt}\right)_{dyn} = \left(\frac{dM}{dt}\right)_{inviscid} + \left(\frac{dM}{dt}\right)_{diff}. \quad (4)$$

The first term on the right-hand side of (4) is the tendency of AAM due to ‘inviscid dynamics’ or more precisely, dynamics without any explicit diffusion operators which is accounted for in the second term. Explicit diffusion in the CAM-SE model the fourth-order hyperviscosity on all prognostic variables and additional divergence damping.

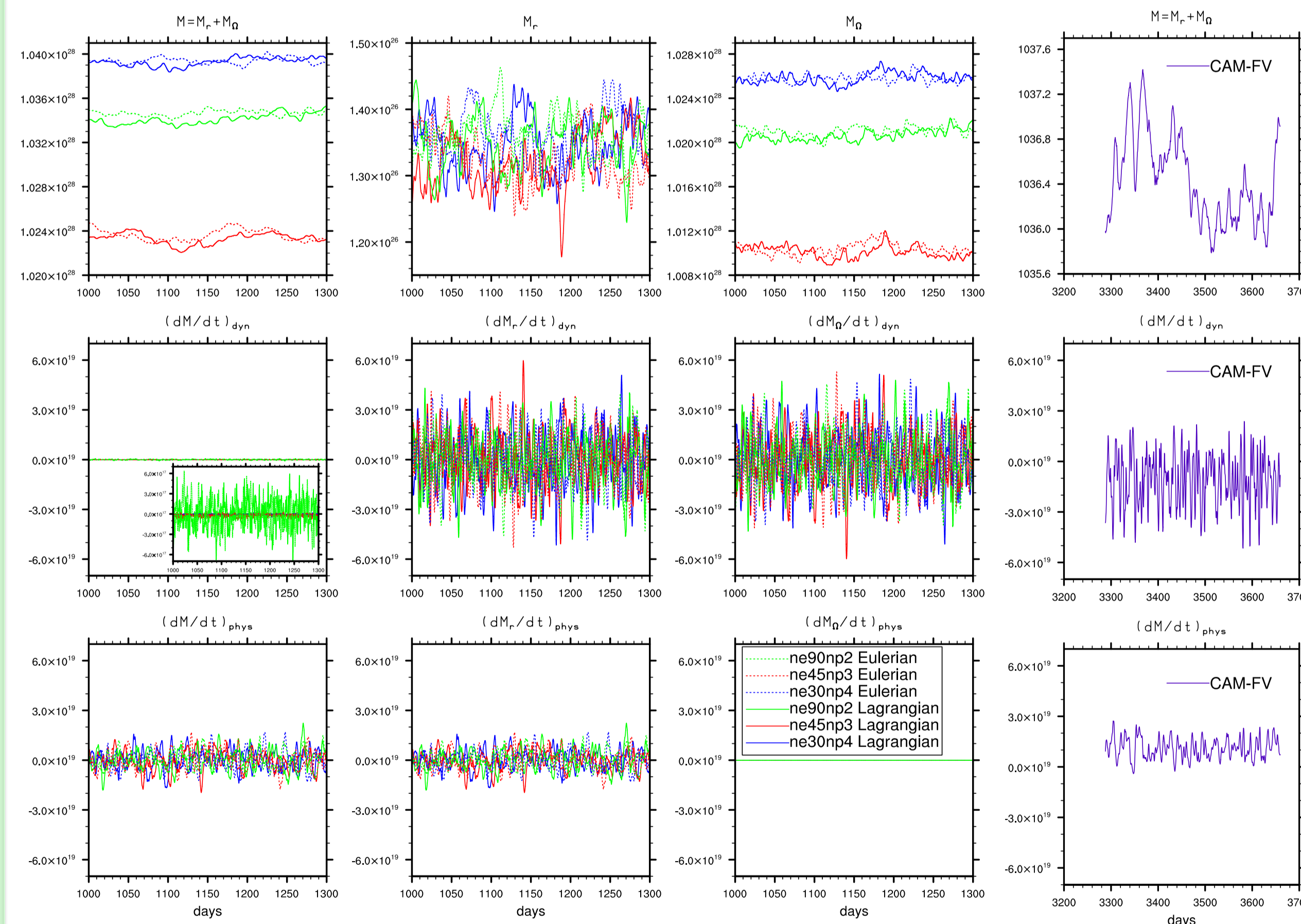


**Figure 1.** First row depicts total or absolute AAM ( $M$ , column 1), the  $\Omega$  AAM ( $M_\Omega$ , column 2), and relative AAM ( $M_r$ , column 3) as a function of time (day 1000 to 1300) for different polynomial orders and vertical advection schemes. Rows two and three show time-tendencies of AAM due to the dynamical core ( $\left(\frac{dM}{dt}\right)_{dyn}$ ) and physical parameterizations ( $\left(\frac{dM}{dt}\right)_{phys}$ ), respectively, with the same partitioning as row one.

## Notation

- ne30np4: standard one degree CAM-SE configuration (30x30 elements per panel, 4x4 quadrature points, third-order polynomial basis functions)
- ne45np3: one degree CAM-SE but with second-order polynomials
- ne90np2: one degree CAM-SE but with first-order polynomials
- For comparison we also show CAM-FV (finite-volume) results from Lebonnois et al. (2012)

## Summary of results

- CAM-FV has very large spurious sources/sinks of AAM in the dynamical core (same size as physical sources/sinks!)
- All CAM-SE configurations conserve AAM very well: dynamics tendencies are about 3 orders of magnitude smaller than the physical AAM tendencies
- >  $dM/dt$  from dynamics compensates almost perfectly the fluctuations of mass during advection ( $dM_\Omega/dt$ ).
- > In the breakdown of the dynamics contributions into inviscid dynamics and hyper-viscosity (Figure 2), we see that tendencies are largest for hyper-viscosity (about a factor 10 or more than inviscid dynamics).
- Are the excellent AAM conservation properties due to high-order numerical methods?
- > CAM-SE was run at the same horizontal resolution but with lower-order polynomials
- > Conservation properties degrade slightly but the spurious AAM sources/sinks are still very small compared to the physical sources/sinks.
- The floating Lagrangian coordinate version of CAM-SE conserves AAM slightly less well compared to the Eulerian vertical coordinate version.

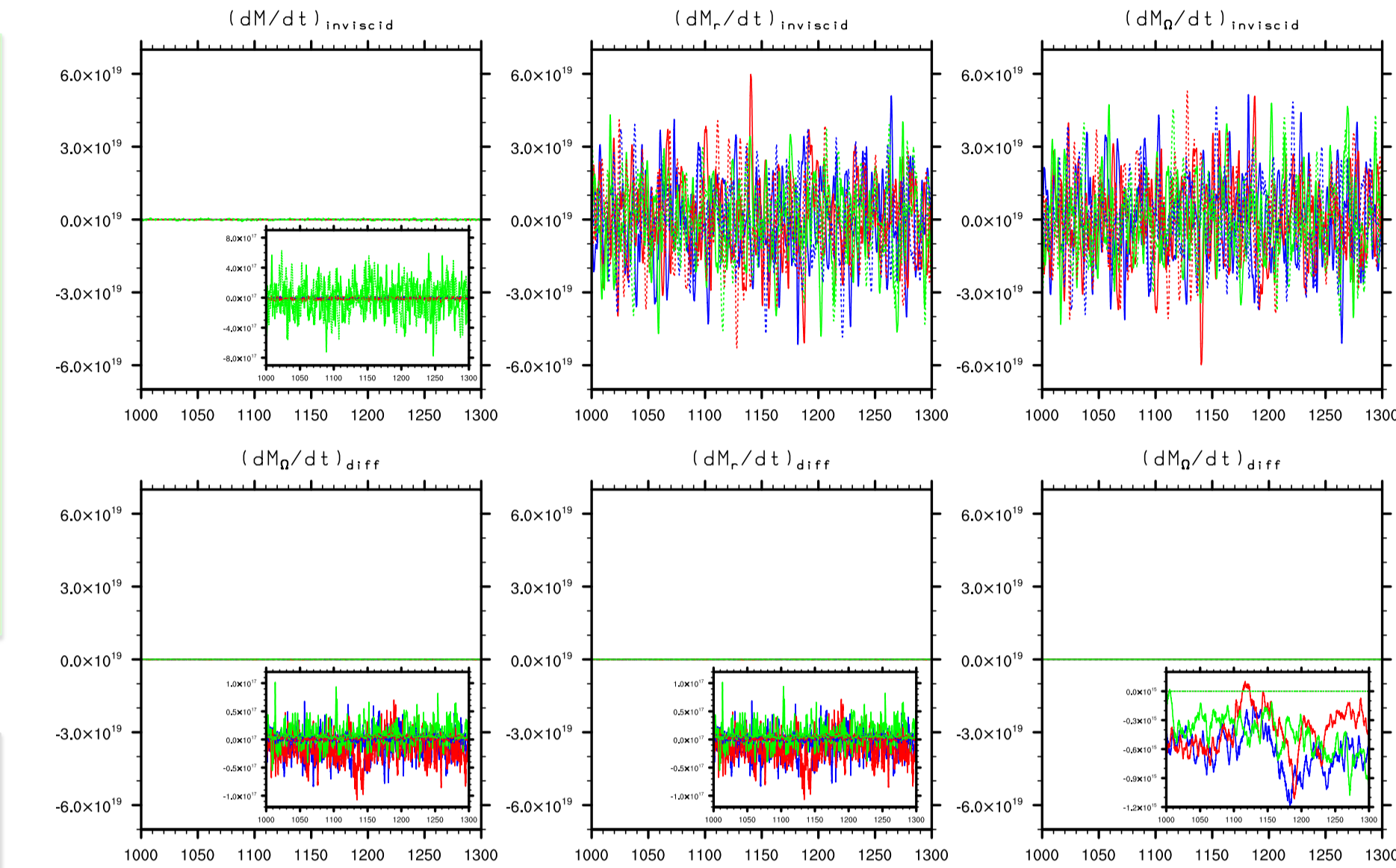


**Figure 2.** Same as Figure 1 but for the ‘inviscid’ part of the dynamical core solver and explicit diffusion operators.

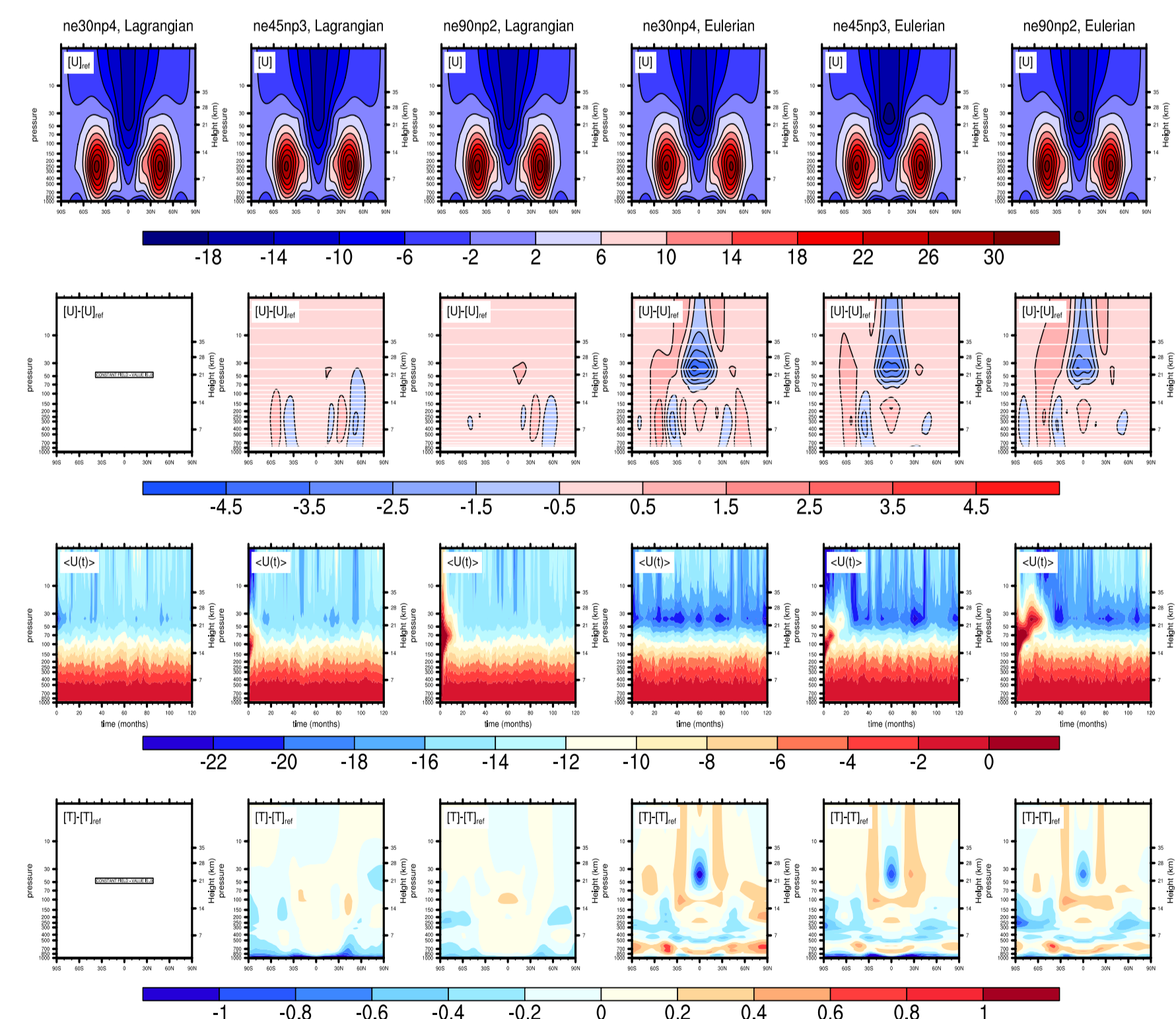


**Figure 3.** First, second, and fourth row are zonal mean quantities averaged over year 3-10 of the simulation for different model configurations; columns from left to right are Lagrangian vertical coordinate configurations at ne30np4, ne45np3, ne90np2 followed by Eulerian vertical coordinate configurations in the same order. First row is zonal mean zonal winds ( $[u]$ ) and the second row is the difference between  $[u]$  for the configuration in question and  $[u]$  for the ne30np4 Lagrangian configuration. Third row is time-height plots of monthly-mean, zonal-mean zonal wind averaged between 6°N and 6°S. Fourth row is the same as the second row but for temperature. The horizontal white lines on row two mark the location of the mid-levels. Note that the three upper most layers are sponge layers with increased explicit and implicit numerical diffusion.